

## Renormalized multiple-scattering theory of photoelectron diffraction

M. Biagini

*Dipartimento di Fisica, Università di Modena, via Campi 213/a, I-41100 Modena, Italy*

(Received 29 May 1992; revised manuscript received 1 February 1993)

The current multiple-scattering cluster techniques for the calculation of x-ray photoelectron and Auger-electron diffraction patterns consume much computer time in the intermediate-energy range (200–1000 eV); in fact, because of the large value of the electron mean free path and of the large forward-scattering amplitude at such energies, the electron samples a relatively large portion of the crystal, so that the number of paths to be considered becomes dramatically high. An alternative method is developed in the present paper: instead of calculating the individual contribution from each single path, the scattering matrix of each plane parallel to the surface is calculated with a renormalization process that calculates every scattering event in the plane up to infinite order. Similarly the scattering between two planes is calculated up to infinite order, and the double-plane scattering matrix is introduced. The process may then be applied to the calculation of a larger set of atomic layers. The advantage of the method is that a relatively small number of internuclear vectors have been used to obtain convergence in the calculation.

### I. INTRODUCTION

In recent years x-ray photoelectron diffraction (XPD) and Auger-electron diffraction (AED) have been applied by many authors to the study of the structure of solid surfaces and interfaces.<sup>1</sup> This technique is based on the fact that the electrons photoejected may undergo elastic scattering from the atoms of the crystal, so that the interference between the direct and the scattered waves gives origin to diffraction patterns. Besides, since all elements have a unique photoelectron spectrum, it is almost always possible to find a kinetic energy specific for each element of the system under consideration, and to localize the origin of the signal in different sites of the crystal, so that different features of the system may be emphasized. The current way to obtain structural information about the sample is to monitor the intensity of the photoelectron current as a function of the emission direction relative to the crystal axis: this may be done both through azimuthal and polar scanning; another possibility consists in varying the energy of the incoming photon by keeping fixed the geometry of the experiment. The specific advantage of these techniques is that they probe the short-range order as it is seen from a certain type of atom in the crystal; this makes these local diffraction methods complementary to low-energy electron diffraction (LEED) and x-ray diffraction, which are sensitive to the long-range order. Besides XPD and AED have been successfully applied to the study of the passivation of GaAs(001) surfaces by incorporation of group-VI atom,<sup>2</sup> a situation for which other techniques were revealed to be inadequate. The large variations in the intensities of XPD and AED patterns are originated by two different physical processes; some peaks coincide with the directions of the internuclear axis of the emission site and its neighbors: these peaks are originated by the forward-focusing effect that is observed above a few hundreds eV and produces an intensity enhancement approaching a

finite limit as the kinetic energy of the ejected electron tends to infinity.<sup>3</sup> All the other peaks are bound to specific diffraction effects. Their angular position depends strongly on the kinetic energy of the photoelectron so that their analysis requires an adequate mathematical treatment. The basic physical process for the explanation of photoelectron diffraction patterns is the elastic electron scattering. Core-level photoabsorption gives origin to an atomiclike outgoing electron wave: this wave may directly reach the detector, or it may be elastically scattered by the atoms in the crystal. The interference effect among the different electron waves depends essentially on the difference in path lengths, so that the diffraction pattern is strictly bound to the geometry of the system. In favorable cases single-scattering calculations have proved to describe accurately the chief features of the experimental data, but they are inadequate for the full analysis of most experiments, so that a multiple-scattering theory becomes necessary. The multiple-scattering approach consists of a perturbative expansion in the strength of the scattering potential, which may be expressed in terms of the hypothetical paths that the electron follows as it scatters and propagates from atom to atom. The single-scattering theory is obtained by the truncation of the perturbative series at the first order; however, because of the relatively large values of the atomic scattering factors, higher-order perturbative terms must be, in general, considered. The first multiple-scattering approach to angle-resolved photoemission was presented by Li, Lubinsky, and Tong<sup>4</sup> but the sophistication of these calculations has limited their use for the simulation of experimental data. A more recent approach to the multiple-scattering problem was presented by Barton, Robey, and Shirley;<sup>5</sup> they consider the terms in the perturbative expansion by summing each term after verifying that its contribution was not inferior to the selected amplitude cutoff value. They applied their theory only to the case of photoemission from an *S*-core level and introduced curved-wave correc-

tions through the Taylor-series magnetic-quantum-number expansion.<sup>6</sup> Rehr and Albers<sup>7</sup> have recently presented an alternative theory based on a separable decomposition of the free-electron Green's function. This theory has been recently applied by Osterwalder *et al.* for the simulation of XPD patterns for Ni $2p_{3/2}$  emission from a Ni(001) substrate.<sup>8,9</sup> Most of the multiple-scattering simulations for XPD and AED have been executed by cluster calculation techniques; these methods are, however, time consuming as soon as the number of atoms and the order of scattering are increased. An alternative method is developed in the present paper: instead of calculating the individual contribution from each single path, the scattering matrix of each plane parallel to the surface is calculated with a renormalization process which includes every scattering event in the plane up to infinite order for a selected set of internuclear vectors; the scattering between two planes is then calculated up to infinite order so that the double-plane scattering matrix is introduced, etc. The computation time depends strongly on the number of internuclear vectors utilized, but it has been found that a relatively small number of internuclear vectors is sufficient to obtain a convergent solution. The present method is conceptually similar to those applied in LEED theories:<sup>11</sup> in fact, the scattering processes are calculated first on a single layer, then in a couple of layers, and finally among couples of layers. However, the mathematical treatment is very different; in fact, in LEED theories the vectors used in the calculation are reciprocal-lattice vectors, while in the present theory, the vectors considered are internuclear vectors. This difference is originated by the fact that, in the case of photoelectron diffraction, the origin of the incident electron wave is located inside the crystal, so that it cannot be described as a plane wave; this implies that atoms with different distances from the emitter are not equivalent, while all atoms in the same plane, parallel to the surface, are equivalent in the case of LEED theories. This lack of translational symmetry is one of the main differences between photoelectron diffraction and low-energy electron diffraction.

## II. GENERAL THEORY

The angle-resolved cross section for the photoelectron diffraction process may be calculated through the perturbation theory; the wave function in the position  $\mathbf{R}$ , far from the crystal, may be expanded in a perturbative series in the strength of the atomic scattering potential:<sup>9</sup>

$$\psi(\mathbf{R}) = \psi_0(\mathbf{R}) + \psi_1(\mathbf{R}) + \psi_2(\mathbf{R}) + \dots, \quad (1)$$

where the zero order term  $\psi_0$  has the following form:

$$\begin{aligned} \psi_0(\mathbf{R}) = & \frac{\exp(ikR)}{ikR} e^{-L(0)/2\lambda} \\ & \times \sum_{l_f=l_i\pm 1} (-i)^{l_f} \exp(i\sigma_{l_f}) \langle Y_{l_f m} | Y_{10} | Y_{l_i m} \rangle \\ & \times I_{l_f} \sqrt{4\pi} Y_{l_f m}(\theta_{\mathbf{R}}, \phi_{\mathbf{R}}), \end{aligned} \quad (2)$$

where  $\mathbf{k}$  is the electron final wave vector,  $l_i$  and  $l_f$  are, respectively, the initial and final angular momenta,  $\theta_{\mathbf{R}}$  and  $\phi_{\mathbf{R}}$  are the polar coordinates of  $\mathbf{R}$  in a reference system where the  $z$  axis coincides with the polarization vector of the incident photon;  $\sigma_l$  are the phase shifts related to the short-range central potential of the ionized atom (the long-range Coulomb field is neglected<sup>12</sup>),  $I_{l_f}$  is the integral corresponding to the radial component of the wave function and is given by

$$I_{l_f} = \int R_{nl}(r) R_{El}(r) r^3 dr, \quad (3)$$

while

$$\begin{aligned} \langle Y_{l_f m} | Y_{10} | Y_{l_i m} \rangle \equiv & \int Y_{l_f m}^*(\theta, \phi) Y_{10}(\theta, \phi) \\ & \times \sin\theta \cos\theta d\theta d\phi. \end{aligned} \quad (4)$$

The electron mean free path  $\lambda$  expresses the attenuation of the electron wave due to inelastic processes, such as plasmon losses, single-particle excitations, etc.;  $L(0)$  is the distance traveled by the electron before reaching the exit surface. The single-scattering term  $\psi_1$  is given by

$$\begin{aligned} \psi_1(\mathbf{R}) = & \frac{\exp(ikR)}{ikR} \sum_{l_f=l_i\pm 1} (-i)^{l_f} \exp(i\sigma_{l_f}) \langle Y_{l_f m} | Y_{10} | Y_{l_i m} \rangle I_{l_f} \sum_{i \neq 0} \sqrt{4\pi} Y_{l_f m}(\theta_{\mathbf{a}_i}, \phi_{\mathbf{a}_i}) c_{l_f}(ka_i) \\ & \times P(\mathbf{a}_i, \mathbf{R}) f(\mathbf{a}_i, \mathbf{R}, \theta_{\mathbf{a}_i, \mathbf{R}}) \exp[-L(\mathbf{a}_i)/2\lambda], \end{aligned} \quad (5)$$

where

$$P(\mathbf{a}_i, \mathbf{R}) = \frac{1}{a_i} \exp[-a_i/(2\lambda) + ik a_i (1 - \cos\theta_{\mathbf{a}_i, \mathbf{R}})], \quad (6)$$

the vector  $\mathbf{a}_i$  is the internuclear separation between the photoemitter and the scattering atom, and  $f(a, b, \theta)$  is the effective curved-wave scattering amplitude,<sup>7</sup> given by

$$f(a, b, \theta) = \frac{1}{k} \sum_l (2l+1) t_l c_l(ka) c_l(kb) P_l(\cos\theta). \quad (7)$$

In Eq. (7)  $t_l = \exp(i\delta_l) \sin(\delta_l)$  are the components of the atomic  $t$  matrix,  $P_l(\cos\theta)$  is a Legendre polynomial of order  $l$ , and  $c_l$  are dimensionless polynomial factors, related to the spherical Hankel functions by the following relation:

$$h_l^+(x) = i^{-l} \frac{e^{ix}}{x} c_l(x) \quad (8)$$

[note that the  $\delta_l$  phase shift differs from the  $\sigma_l$  phase shift, introduced in Eq. (2), when atomic relaxation effects are introduced in the calculation of  $\sigma_l$ ]. The effective curved-wave scattering factors (7) may be obtained if one truncates the Rehr-Albers scattering matrices  $F_{\lambda,\lambda'}$  to lowest order;<sup>7</sup> this approximation has proved to be adequate for kinetic energies above a few hundreds eV, but it may not give fully accurate results for the forward-scattering directions in the high-energy range.<sup>10</sup> This fact may be observed for emission directions along the principal axis of the crystal, where the atoms are more close to each other (the curved-wave

corrections rapidly diminish when the distance between the atoms is increased). However, interesting features, bound to specific diffraction effects which may give important information about the surface structure and interatomic distances, may be evidenced for different emission directions (in an azimuthal scanning, e.g., it is sufficient to choose a polar angle which does not lie along one of the few principal axis directions). The present method is then more accurate for the study of XPD peaks, whose angular position does not coincide with the crystal principal axis directions. The  $n$ th scattering term has the following form:

$$\begin{aligned} \psi_n(\mathbf{R}) = & \frac{\exp(ikR)}{ikR} \sum_{l_f=l_i \pm 1} (-i)^{l_f} \exp(i\sigma_{l_f}) \langle Y_{l_f m} | Y_{10} | Y_{l_f m} \rangle I_{l_f} \\ & \times \sum_{\substack{i_1, i_2, \dots \\ i_1 \neq 0, \\ i_2 \neq i_1, \dots}} \sqrt{4\pi} Y_{l_f m}(\theta_{\mathbf{a}_{i_1}}, \phi_{\mathbf{a}_{i_1}}) c_{l_f}(ka_{i_1}) \\ & \times P(\mathbf{a}_{i_1}, \mathbf{R}) f(a_{i_1}, a_{i_2}, \theta_{\mathbf{a}_{i_1} \mathbf{a}_{i_2}}) \times \dots \times P(\mathbf{a}_{i_n}, \mathbf{R}) f(a_{i_n}, R, \theta_{\mathbf{a}_{i_n} \mathbf{R}}) \\ & \times \exp[-L(\mathbf{a}_{i_1} + \dots + \mathbf{a}_{i_n})/2\lambda]. \end{aligned} \quad (9)$$

Some useful notations are now introduced: if  $\mathbf{b}$  is an internuclear vector, the double-scattering event for an electron coming along the internuclear direction  $\mathbf{a}$ , scattered first along  $\mathbf{b}$ , and then along  $\mathbf{c}$ , may be expressed through

$$R_{\mathbf{b}}(\mathbf{c}) \equiv P(\mathbf{b}, \mathbf{R}) f(b, c, \theta_{bc}), \quad (10)$$

so that, if the incident electron wave function is  $\psi_i$ , the wave function  $\psi_f$  for an electron coming out along  $\mathbf{c}$ , after the two scattering events, is given by the following expression:

$$\psi_f = \psi_i f(a, b, \theta_{ab}) R_{\mathbf{b}}(\mathbf{c}). \quad (11)$$

All the multiple-scattering events on a plane parallel to the surface can similarly be expressed through

$$S(\mathbf{a}, \mathbf{c}) \equiv f(a, c, \theta_{ac}) + \sum_{i_1} f(a, b_{i_1}, \theta_{ab_{i_1}}) \left[ R_{\mathbf{b}_{i_1}}(\mathbf{c}) + \sum_{i_2} R_{\mathbf{b}_{i_1}}(\mathbf{b}_{i_2}) [R_{\mathbf{b}_{i_2}}(\mathbf{c}) + \dots] \dots \right], \quad (12)$$

where the sums are intended over a set of internuclear vectors  $\mathbf{b}_i$ , lying in the plane. Equation (12) has been derived with the hypothesis of two-dimensional periodicity in the layer; however, since the wave function is exponentially damped, such periodicity is actually required only for a region whose extension is of the order of the electron mean-free-path length. If the two-dimensional unit cell contains more than one atom, Eq. (12) applies to the sublattices corresponding to each atom in the unit cell, while the scattering between sublattices may be calculated likewise the scattering among different layers (see below). The multiple-scattering problem in a plane parallel

to the surface may then be calculated up to the infinite order; in fact,  $R_{\mathbf{b}_i}(\mathbf{b}_j)$  may be represented as a matrix  $R_j^i$ , so that Eq. (12) can be written in the form

$$\begin{aligned} S(\mathbf{a}, \mathbf{c}) = & f(a, c, \theta_{ac}) \\ & + F_i^a [R_c^i + R_j^i [R_c^j + R_k^j [R_c^k + \dots] \dots]] \\ = & f(a, c, \theta_{ac}) + F_i^a [1 + R + R^2 + R^3 + \dots]_j^i R_c^j \\ = & f(a, c, \theta_{ac}) + F_i^a \left[ \frac{1}{1-R} \right]_j^i R_c^j; \end{aligned} \quad (13)$$

where

$$F_i^a \equiv f(a, b_i, \theta_{ab_i}), \quad (14)$$

$$R_c^i \equiv R_{b_i}(\mathbf{c}). \quad (15)$$

The multiple-scattering problem for a plane parallel to the surface is then resolved up to the infinite order, by inversion of the matrix  $R$ . If the plane under consideration contains the ionized atom, the first event is the absorption of the incoming photon so that Eq. (13) must be modified and becomes

$$S^0(\epsilon, \mathbf{c}) = \sum_{l_f=l_i \pm 1} (-i)^{l_f} \exp(i\sigma_{l_f}) \langle Y_{l_f m} | Y_{10} | Y_{l_i m} \rangle I_{l_f} \left[ \sqrt{4\pi} Y_{l_f m}(\theta_{\epsilon c}, \phi_{\epsilon c}) c_1(kc) + U_i^{\epsilon, l_f} \left[ \frac{1}{1-R} \right]_j^i R_c^j \right], \quad (16)$$

where

$$U_i^{\epsilon, l_f} \equiv \sqrt{4\pi} Y_{l_f m}(\theta_{\epsilon a_i}, \phi_{\epsilon a_i}) c_{l_f}(ka_i). \quad (17)$$

In the case  $\mathbf{c}$  coincides with  $\mathbf{R}$ ,  $S^0(\epsilon, \mathbf{R})$  gives the electron wave-function amplitude at the detector for the multiple-scattering problem corresponding to one single atomic layer. The scattering events between two planes parallel to the surface, may be described with a similar treatment; it is necessary to define four two-plane scattering matrices  $S_{1,1}$ ,  $S_{1,2}$ ,  $S_{2,1}$ ,  $S_{2,2}$ , where  $S_{i,j}$  refers to the case where the first scattering event is in the plane  $i$  and the last one is in the plane  $j$ . The scattering processes may be summarized as follows: (a) the electron enters the plane  $i$ , travels in the plane, and then exists along the final vector  $\mathbf{c}$ ; (b) the electron enters the plane  $i$ , it is scattered here until it exits towards the plane  $j$  along an internuclear vector  $\mathbf{b}_i$ , it travels in the plane  $j$ , and then exists along  $\mathbf{c}$ ; etc. These processes may be expressed as follows:

$$S_{1,1}(\mathbf{a}, \mathbf{c}) = S(\mathbf{a}, \mathbf{c}) + S_i^a(P_{12})_j^i S_k^j(P_{21})_i^k [S_c^i + S_i^i(P_{12})_j^i S_k^j(P_{21})_i^k [S_c^i + \dots] \dots], \quad (18)$$

where the sums over the repeated index are omitted,  $S_j^i \equiv S(\mathbf{b}_i, \mathbf{b}_j)$ ,  $S_j^a \equiv S(\mathbf{a}, \mathbf{b}_j)$ ,  $S_c^i \equiv S(\mathbf{b}_i, \mathbf{c})$ , and  $P_{ij}$  is the matrix corresponding to the propagation of the electron from the plane  $i$  to the plane  $j$  and is given by the following expression:

$$(P_{ij})_n^m = \delta_{m,n} \frac{\exp[ikb_n(1 - \cos\theta_{b_n R}) - b_n/2\lambda]}{b_n}, \quad (19)$$

where  $\mathbf{b}_n$  is an internuclear scattering vector from the plane  $i$  to the plane  $j$ . All the possible scattering processes over each plane are already included through the matrix  $S$ , and the scattering between the two planes may be evaluated up to the infinite order, by simply summing the geometric series. One has

$$S_{1,1}(\mathbf{a}, \mathbf{c}) = S(\mathbf{a}, \mathbf{c}) + (SP_{12}SP_{21})_i^a \left[ \frac{1}{1-SP_{12}SP_{21}} \right]_j^i S_c^j. \quad (20)$$

The other three two-plane scattering matrices have similar expressions:

$$\begin{aligned} S_{1,2}(\mathbf{a}, \mathbf{c}) &= (SP_{12})_i^a \left[ \frac{1}{1-SP_{21}SP_{12}} \right]_j^i S_c^j, \\ S_{2,1}(\mathbf{a}, \mathbf{c}) &= (SP_{21})_i^a \left[ \frac{1}{1-SP_{12}SP_{21}} \right]_j^i S_c^j, \\ S_{2,2}(\mathbf{a}, \mathbf{c}) &= S(\mathbf{a}, \mathbf{c}) + (SP_{21}SP_{12})_i^a \left[ \frac{1}{1-SP_{21}SP_{12}} \right]_j^i S_c^j. \end{aligned}$$

The two-plane scattering matrices may be written in a more compact form, as a single matrix  $\tilde{S}$ ,

$$\tilde{S} \equiv \begin{vmatrix} S_{1,1} & S_{1,2} \\ S_{2,1} & S_{2,2} \end{vmatrix}, \quad (21)$$

which may be also written in the following expression:

$$\tilde{S} = \begin{vmatrix} S & 0 \\ 0 & S \end{vmatrix} + \begin{vmatrix} 0 & SP_{12} \\ SP_{21} & 0 \end{vmatrix} \left[ 1 - \begin{vmatrix} 0 & SP_{12} \\ SP_{21} & 0 \end{vmatrix} \right]^{-1} \begin{vmatrix} S & 0 \\ 0 & S \end{vmatrix}, \quad (22)$$

as one can easily prove. The multiple-scattering solution for a system with only two planes has the following form:

$$\psi(\mathbf{R}) \propto S^0(\epsilon, \mathbf{R}) + \sum_i S^0(\epsilon, \mathbf{b}_i) P_{12}(\mathbf{b}_i) [S_{2,1}(\mathbf{b}_i, \mathbf{R}) e^{-L(1)/2\lambda} + S_{2,2}(\mathbf{b}_i, \mathbf{R}) e^{-L(2)/2\lambda}], \quad (23)$$

where the sum is intended over the internuclear vectors between the two planes. The scattering among a higher number of planes may be calculated similarly: however, since the dimensions of the  $n$ -plane scattering matrix are proportional to the number of planes  $n$ , it has been found more convenient, from a computational point of view, to introduce the

scattering among couples of planes sequentially up to a finite order, instead of following the same procedure used for the two-plane scattering matrix. For more clarity I show explicitly how the scattering processes between two couples of planes (indicated as couple  $a$  and couple  $b$ ) may be calculated up to third order. Suppose for simplicity an electron incident on the couple of planes  $a$  along an internuclear vector  $\mathbf{a}$ ; the processes to be inserted in the calculations are the following: (a) the electron is scattered by couple  $a$  towards the detector; (b) the electron is scattered by couple  $a$  towards couple  $b$  and then by couple  $b$  towards the detector; (c) the electron is scattered by couple  $a$  towards couple  $b$ , then it is scattered by couple  $b$  towards couple  $a$  and finally by couple  $a$  towards the detector. All these processes may be described by the following mathematical expression:

$$\tilde{S}^{(a)}(\mathbf{a}, \mathbf{R}) + \sum_{\mathbf{b}_i} \tilde{S}^{(a)}(\mathbf{a}, \mathbf{b}_i) P(\mathbf{b}_i, \mathbf{R}) \left[ \tilde{S}^{(b)}(\mathbf{b}_i, \mathbf{R}) + \sum_{\mathbf{c}_j} \tilde{S}^{(b)}(\mathbf{b}_i, \mathbf{c}_j) P(\mathbf{c}_j, \mathbf{R}) \tilde{S}^{(a)}(\mathbf{c}_j, \mathbf{R}) \right], \quad (24)$$

where  $\tilde{S}^{(a)}$  and  $\tilde{S}^{(b)}$  are, respectively, the two-plane scattering matrix for the couples of planes  $a$  and  $b$ , given by Eqs. (21) or (22),  $\mathbf{R}$  is the direction of emission towards the detector,  $P(\mathbf{b}, \mathbf{R})$  is given by Eq. (6), and the sums over  $\mathbf{b}_i$  and over  $\mathbf{c}_j$  are intended over all internuclear vector between the two couples  $a$  and  $b$ . Note that every possible scattering event within each couple of planes is implicitly calculated, since the scattering matrices  $\tilde{S}^{(a)}$  and  $\tilde{S}^{(b)}$  have been already renormalized. For each emission direction,  $\mathbf{R}$  is fixed so that  $\tilde{S}^{(a)}(\mathbf{b}_i, \mathbf{R})$  and  $\tilde{S}^{(b)}(\mathbf{c}_j, \mathbf{R})$  may be regarded as vectors instead of a matrix; at each step in the calculation of Eq. (24), one has then to multiply a vector by a matrix and not a matrix by a matrix, so that the number of terms to be computed reduces to  $n$  instead of  $n^2$ , if  $n$  is the vector dimension. This method has been applied to the study of different solid surfaces: a set of eight atomic layers has been considered and the scattering among couples of planes has been introduced up to fourth order. The photoelectron intensity then has the following form:

$$I_{l,m} \propto \left| \sum_{l_f=l_i \pm 1} (-i)^{l_f} \exp(i\sigma_{l_f}) \langle Y_{l_f m} | Y_{10} | Y_{l_i m} \rangle I_{l_f} \left[ \sqrt{4\pi} Y_{l_f m}(\theta_{\mathbf{R}}, \phi_{\mathbf{R}}) + \sum_{i \neq 0} \sqrt{4\pi} Y_{l_f m}(\theta_{\mathbf{a}_i}, \phi_{\mathbf{a}_i}) c_{l_f}(ka_i) S^{(8)}(\mathbf{a}_i, \mathbf{R}) \right] \right|^2, \quad (25)$$

where  $S^{(8)}(\mathbf{a}, \mathbf{R})$  is the eight-plane scattering matrix, which is independent of the position of the photoemitter from the angular momentum  $l_f$  and from the polarization of the incident photon; this fact is very useful from a computational point of view, since the multiple-scattering calculation must be executed only once, while the result is valid for all inequivalent emitters, angular momentum  $l_f$ , and polarization vectors. If the spin-orbit coupling is neglected, Eq. (25) must be summed over all possible values of the magnetic quantum number  $m$ . When the spin-orbit coupling is introduced, the initial state is represented by a spin orbital of one of the following forms:

$$|j=l+\frac{1}{2}, m_j\rangle = \begin{pmatrix} \left[ \frac{l+m_j+1/2}{2l+1} \right]^{1/2} \psi_{l, m_j - \frac{1}{2}} \\ \left[ \frac{l-m_j+1/2}{2l+1} \right]^{1/2} \psi_{l, m_j + \frac{1}{2}} \end{pmatrix}, \quad (26)$$

$$|j=l-\frac{1}{2}, m_j\rangle = \begin{pmatrix} - \left[ \frac{l-m_j+1/2}{2l+1} \right]^{1/2} \psi_{l, m_j - \frac{1}{2}} \\ \left[ \frac{l+m_j+1/2}{2l+1} \right]^{1/2} \psi_{l, m_j + \frac{1}{2}} \end{pmatrix}. \quad (27)$$

As a final state, one must consider the two possibilities of spin-up and spin-down electron states, which are equivalent when the spin-orbit coupling is neglected; the intensity is then given by

$$I = \sum_{m_j=-l-1/2}^{l+1/2} \left[ \frac{l+m_j+1/2}{2l+1} I_{l, m_j - 1/2} + \frac{l-m_j+1/2}{2l+1} I_{l, m_j + 1/2} \right] = \frac{2l+2}{2l+1} \sum_{m=-l}^l I_{lm}, \quad (28)$$

for  $j=l+\frac{1}{2}$ , and similarly for  $j=l-\frac{1}{2}$ .

### III. NUMERICAL RESULTS

In this section the theory described above is applied to the study of emission from a semi-infinite substrate. In contrast to the case of emission from adsorbate structures, this case presents greater difficulties from a computational point of view: in fact, the number of important scatterers is larger and many nonequivalent emitters with a different local environment and varying distance to the surface must be considered. For a typical cluster technique this situation results to be complex, since the calculation must be executed from the beginning for every nonequivalent emitter. The present method overcomes this difficulty, since the multiple-scattering calculation is evaluated only once, while the result is used for all emitters, as results from Eq. (25); the contribution from several hundreds of atoms is included in the present calculation of the photocurrent intensity. Multiple-scattering calculations for photoemission from a Ni(001) surface have been executed for small clusters of  $\approx 40$

atoms by Fadley and co-workers,<sup>8,9</sup> while Fritzsche has presented multiple-scattering calculations only up to the third order, for Auger-electron emission from a Ni(111) surface.<sup>13</sup> The multiple-scattering calculation presented refers to the case of Ni2*p* emission from a Ni(001) substrate at a kinetic energy  $E=630$  eV: the incident beam is supposed unpolarized, so that two orthogonal photon polarization vectors have been considered. Both *s*- and *d*-channel contributions have been evaluated and 20 phase shifts have been used for the calculation of the ion-core scattering factor. An azimuthal scanning at a fixed polar angle  $\theta=16^\circ$  have been considered: the great importance of multiple-scattering processes is shown in Fig. 1, where multiple-scattering (solid line) and single-scattering (dashed line) curves are represented. At such a polar angle, the emission direction never coincides with directions connecting the emitter with overlying nearest- or next-nearest-neighbor atoms, so that the forward-focusing effect is not evident from a simple inspection of the diffraction pattern. All the peaks in Fig. 1 are then originated by complex diffraction processes, so that it is not possible to give a simple explanation of the great differences between the single-scattering and multiple-scattering curves. In Fig. 2 the convergence in the internuclear vectors is illustrated. An increasing number of internuclear vectors have been introduced: more precisely, all the internuclear vectors smaller than 5, 8, and 11 Å have been, respectively, used in the multiple-scattering calculation for the dash-dotted, dashed, and solid lines. The matrix dimensions involved in the calculation obviously depend on the number of internuclear vectors; for example, the one-plane scattering matrix dimensions are  $10 \times 10$ ,  $32 \times 32$ , and  $54 \times 54$ , respectively, for the dash-dotted, dashed, and solid lines. Unlike the single-scattering curve, the dash-dotted curve in Fig. 2, though obtained by using a small number of internuclear vectors, reproduces rather well the convergent solution: the only differences consist in a lowering of the peak at  $21^\circ$  and in the presence of the broad peak at  $38^\circ$ , which is present also in the single-scattering curve, while all the other structures, even the minor ones, are well reproduced. In

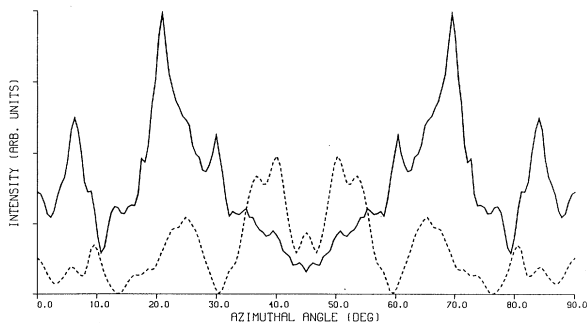


FIG. 1. Comparison between multiple-scattering (solid line) and single-scattering (dashed line) calculations for Ni2*p* emission from a Ni(001) substrate at a kinetic energy  $E=630$  eV: the incident beam is supposed unpolarized and the polar angle is set to  $16^\circ$ .

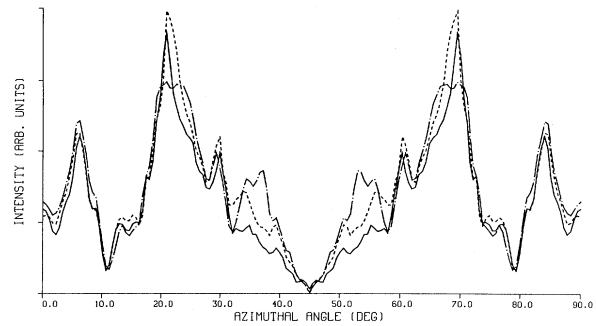


FIG. 2. Convergence in the internuclear vectors: multiple-scattering calculations for the same case as in Fig. 1. All the internuclear vectors smaller than 11, 8, and 5 Å have been, respectively, used for the solid, dashed, dash-dotted lines.

Fig. 1, the differences between the solid and the dashed curves are much smaller with respect to the differences between the dashed and the dash-dotted curves: it results then that the chief contribution to the diffraction pattern arises from the small internuclear vectors; this does not mean, however, that only short total path lengths must be considered, since the electron may be scattered many times before reaching the detector. This fact may be explained as follows: it is well known that diffraction effects are strong when the wavelength of the incident wave is comparable to the lattice constant, while they tend to be averaged out for a wavelength much shorter than the lattice constant. An electron traveling along a path formed by large internuclear vectors interacts with a broader lattice, so that diffraction processes may be weak for this kind of path, since the photoelectron wavelength is considerably smaller than the lattice constant, for energy above a few hundreds eV. A path formed by small internuclear vectors may then present the most important diffraction effects. In Fig. 3 the convergence in the photoemitter depth is illustrated: short-dash-long-dashed, dash-dotted, dashed, and solid lines refer, respectively, to the intensity with emitter in up to two, four, six, and eight atomic layers; the contributions from deeper pho-

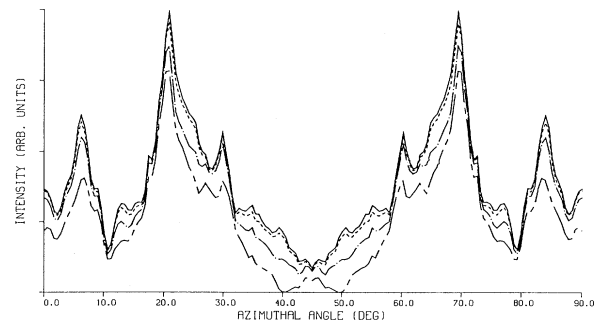


FIG. 3. Convergence in the photoemitter depth: solid, dashed, dash-dotted, and short-dash-long-dashed lines refer, respectively, to the intensity with emitter in up to eight, six, four, and two atomic layers.

toemitters raise considerably the peaks at  $7^\circ$  and at  $30^\circ$ , even if these structures do not coincide with forward-focusing directions. However, it must be stressed that, even in the case when only contributions from emitters in up to two layers are evaluated, scattering events in the whole system are introduced in the calculation, so that such a solution does not represent the effect of the first two layers only.

#### IV. CONCLUSIONS

A multiple-scattering theory for the quantitative calculation of photoelectron and Auger-electron diffraction patterns in the intermediate-energy range (200–1000 eV) has been presented. The ordinary cluster techniques are time consuming when the cluster size and the order of scattering are increased. An alternative method has been developed in the present paper which calculates the contribution of a large number of paths analytically up to infinite order, by a renormalization process. The crucial point of the method consists in the choice of the internuclear vectors to be introduced in the calculation; it has been shown, however, that a relatively small number of internuclear vectors is sufficient to obtain accurate solutions of the problem. This may be explained by the fact that, since the photoelectron wavelength is considerably

smaller than the lattice constant, the diffraction processes become much weaker as the internuclear vectors involved get larger. Nevertheless, paths formed by small internuclear vectors may present important diffraction effects, even for relatively large total length, since the electron may undergo many elastic-scattering processes before reaching the detector because of the relatively large value of the electron mean free path. The curved-wave approximation of Eq. (7), on which the present method is based, is less accurate for the forward-scattering amplitude; this may be observed for emission directions along the principal axis of the crystal, where the focusing and defocusing effect may be evidenced. Although forward focusing is very useful for determining bond directions, it is, in general, not sensitive to bond lengths. One must rely on diffraction modulation away from low index directions to determine the latter. The present method is then more advantageous for the study of XPD peaks, whose angular position does not coincide with the crystal principal axis directions.

#### ACKNOWLEDGMENT

I am very grateful to Professor C. Calandra for several helpful discussions and for the critical reading of the manuscript.

- 
- <sup>1</sup>For a review of photoelectrons techniques see S. A. Chambers, *Adv. Phys.* **40**, 357 (1991); W. F. Egelhoff, Jr., *Crit. Rev. Solid State Mater. Sci.* **16**, 213 (1990).  
<sup>2</sup>S. A. Chambers and V. S. Sundaram, *J. Vac. Sci. Technol.* **B 9**, 2256 (1991).  
<sup>3</sup>H. C. Poon and S. Y. Tong, *Phys. Rev. B* **30**, 6211 (1984); S. Y. Tong, H. C. Poon, and D. R. Snider, *ibid.* **32**, 2096 (1985).  
<sup>4</sup>C. H. Li, A. R. Lubinsky, and S. Y. Tong, *Phys. Rev. B* **17**, 3128 (1978).  
<sup>5</sup>J. J. Barton, S. W. Robey, and D. A. Shirley, *Phys. Rev. B* **34**, 778 (1986).  
<sup>6</sup>J. J. Barton and D. A. Shirley, *Phys. Rev. B* **32**, 1906 (1985).  
<sup>7</sup>J. J. Rehr and R. C. Albers, *Phys. Rev. B* **41**, 8139 (1990).

- <sup>8</sup>J. Osterwalder, A. Stuck, D. J. Friedman, A. Kaduwela, C. S. Fadley, J. Mustre de Leon, and J. J. Rehr, *Phys. Scr.* **41**, 990 (1990).  
<sup>9</sup>A. Kaduwela, D. J. Friedman, and C. S. Fadley, *J. Electron Spectrosc. Relat. Phenom.* **57**, 223 (1991).  
<sup>10</sup>C. S. Fadley, in *Synchrotron Radiation Research: Advances in Surface and Interface Science*, edited by R. Z. Bachrach (Plenum, New York, 1992), Vol. 1, Sec. 3.2, p. 421.  
<sup>11</sup>J. B. Pendry, *Low Energy Electron Diffraction* (Academic, London, 1974), Chap. 4.  
<sup>12</sup>For a discussion of the effect of the Coulomb field see M. Biagini, *Phys. Rev. B* **46**, 10 588 (1992).  
<sup>13</sup>V. Fritzsche, *J. Phys.: Condens. Matter* **2**, 9735 (1990).